1-2014

Novel Computational Approaches Characterizing Knee Physiotherapy

Wangdo Kim
Universidade de Lisboa

Antonio P. Veloso
Universidade de Lisboa

Duarte Araújo
Universidade de Lisboa

Sean S. Kohles
Portland State University

Citation Details

Kim, W., Veloso, A., Araujo, D., and Kohles, S. (2014). Novel Computational Approaches Characterizing Knee Physiotherapy. Journal of Computational Design and Engineering. Volume 1, Issue 1, p, 55-66

Journal of Computational Design and Engineering, Vol. 1, No. 1 (2014) 55~66
www.jcde.org

Novel computational approaches characterizing knee physiotherapy

Wangdo Kim [1], António P. Veloso[1], Duarte Araújo[1] and Sean S. Kohles [2,*]

[1] *Univ Lisboa, Fac Motricidade Humana, CIPER, LBMF, SPERTLAB, Estrada da Costa, P-1499-002, Lisbon, Portugal*
[2] *Division of Biomaterials & Biomechanics, Department of Restorative Dentistry, Oregon Health & Science University, Portland, Oregon, USA*

(Manuscript Received September 28, 2013; Revised November 19, 2013; Accepted November 19, 2013)

Abstract

A knee joint's longevity depends on the proper integration of structural components in an axial alignment. If just one of the components is abnormally off-axis, the biomechanical system fails, resulting in arthritis. The complexity of various failures in the knee joint has led orthopedic surgeons to select total knee replacement as a primary treatment. In many cases, this means sacrificing much of an otherwise normal joint. Here, we review novel computational approaches to describe knee physiotherapy by introducing a new dimension of foot loading to the knee axis alignment producing an improved functional status of the patient. New physiotherapeutic applications are then possible by aligning foot loading with the functional axis of the knee joint during the treatment of patients with osteoarthritis.

Keywords: Instantaneous axes of the knee (IAK); Cylindroidal coordinates; Perception-action coupling manifold; Gibson's theory of affordance; Ball's screw theory; Joachimsthal's equation

1. Introduction

A knee joint's longevity depends on the proper integration of five biomechanical variables: surface congruency, load distribution, stress during loading, contact area, and ligament tension. If some of the functional variables in a specific location are abnormal, the biomechanical system fails, resulting in arthritis. Knee osteotomy is an orthopedic surgical approach to realign the lower limbs by opening or cutting a bone wedge from the femur or tibia. This may be a better alternative than other types of knee replacement surgeries, especially for young people. However, knee osteotomy requires an understanding of the imbalance of stresses at the knee, defining an abnormal gait cycle, and cutting the bone wedge properly. This is a difficult procedure and can cause further damage and/or functional compromise. Indeed, knee osteotomy alone may not generalize most actions of the weight-bearing leg as accomplished by the adaptive movements of all the lower limb joints to the interactive surface.

While some computer-based surgical simulation systems have been developed to help surgeons perform knee surgeries [1], the knee models used are either not patient-specific [2] or lack kinematic and kinetic information [3, 4]. For example, subject-specific simulated [5] knee joint models were created from computed tomography (CT) scans while the subject-specific knee joint kinematics were obtained from fluoroscopic images. The modeling then predicted the medial and lateral tibiofemoral contact forces for different walking trials using static equilibrium in the tibial frontal plane [6].

No efficient method exists for patient-specific knee-model reconstruction [2], contact force computation, or visualization [7]. Furthermore, no system integrates contact-force simulation, gait-cycle simulation, and virtual knee physiotherapy. The use of mathematical models accepted in physiological research is much different from those applied to engineered mechanisms. Constraints are generally realized by rigid links and joints within actual machinery. However, most physiologic joints involve sliding, thus the center of rotation is defined instantaneously.

It is clear that human locomotion may be studied from a number of different points of view, e.g., anatomical, biological, mechanical, etc. Our interest here is in the control of skeletal activities, specifically, the stance phase of gait; when the leg is nearly fully extended and the foot/heal is in contact with a reaction surface. A classical theory of control-based approaches uses the optimization algorithm to fine-tune the muscle excitation patterns for each muscle group and produced a well-coordinated walking pattern that emulated the experimental data [8-10]. However, in order to reduce the number of degrees of freedom (DOFs) upon which the nervous system must operate, we have adopted the proposition that the interaction from the individual and the environment regulates movement though muscle synergies, or groups of

*Corresponding author. Tel.: +1-503-516-7528
E-mail address: Kohles@ohsu.edu

doi: 10.7315/JCDE.2014.006

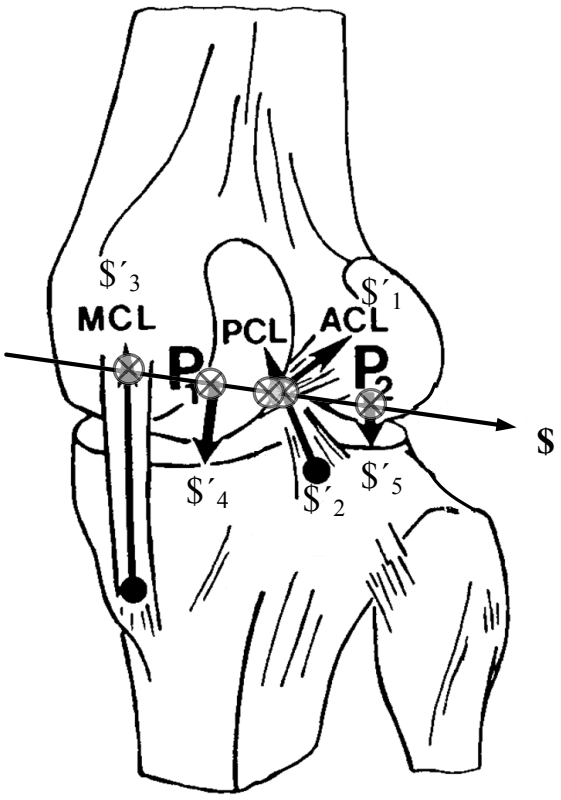

Figure 1. Five constraints $'s are collectively reciprocal to the instantaneous screw axis $. The instantaneous motion of the knee is guided by the constraints of the anterior cruciate ligaments (ACL), posterior cruiciate ligament (PCL), medial collateral ligament (MCL), and articular contact in the medial (P_1) and lateral (P_2) compartments. Note that no combination of the constraint forces that might be generated at the $ will result in a rotation at the $, and no angular velocity about the $ will cause the constraint force to do any work at the points on the medial and lateral contacts. (Adapted from the original figure published in Kim and Kohles [24].)

co-activated muscles, rather than the nervous system controlling individual muscles [11, 12].

In this review, we propose an information based control theory whereby human locomotion is neither triggered nor commanded, but controlled [27, 49]. The basis for this control is the information derived from perceiving oneself in the world [13-16]. Central to this information-based approach will be the observed experimental sensory data [17]. Under the information-based movement control strategies [16], human movement control can be seen as a process that is distributed over the performer-environment system, i.e., rather than being localized in an internal structure associated with the performer [18]. A recent study confirmed that leg stiffness is not directly related to running mechanics, but rather, to the running environment [19]. The performer and his/her environment (the interaction surface) may be said to be co-participants in any resulting action. In this way, actions are specific to function rather than to mechanism [20].

The way that functional movement of a joint is constrained is related both to the location and the direction of its kinetic and kinematic axes. In other words, the kinematic constraints of joints are vector dependent. This in turn implies that constraints may be expressed in terms of linear- rather than point- based geometry as described in screw theory [21, 22]. Screw theory is based on the close relationship between line geometry and spatial kinematics [23]. It has previously been used to characterize knee function [24], explore the effectiveness of a golf club swing [25, 26], and as a method for minimizing interference from motion data. Essentially, symmetry exists between the extent to which a rigid body is constrained and its relative freedom of movement at each instant that a twist is produced.

The aim of this study is to review the foundation of novel computational frameworks for knee physiotherapies that involve the new concept of a perception-action coupling manifold connecting knee kinematics to the ground reaction vector in the sense of a 'reciprocal connection'. Muscle contraction and GRF are compounded into a wrench, which is reciprocal to the instantaneous axes of the knee (IAK) and resolved into component wrenches belonging to the reciprocal screw system. We established a framework for the estimation of reaction of constraints about the knee, in vivo medial and lateral contact force, using a process that is simplified by the judicious generation of IAK for the first order of freedom in equilibrium.

Herein, we discuss how we use data from gait analysis, information-based motion control algorithms, and interactive visualization to assist in knee physiotherapy. Our patient-specific knee informational framework helps us calculate the contact forces at the knee joint and in-turn perform virtual physiotherapy.

2. Materials and methods

2.1 Constructing a patient-specific knee model

Movements and postures are controlled and coordinated to realize functionally specific acts that are themselves based on the perception of affordances, i.e., possibilities for actions [18]. Therefore, during locomotion, we first investigate the complementary nature between the perception of the surface in terms of the ground reaction force (GRF) and the action of the individual in terms of the functional knee joint axes, as perception and action are inseparable [27, 28]. We have previously enunciated a principle which applies to the reciprocal screw system, which involves the theory of equilibrium with a freedom of the first order [15, 29].

It has been shown previously [24] that the forces which constrain the movement of the knee joint through an infinitesimal displacement are interlinked in terms of reciprocal

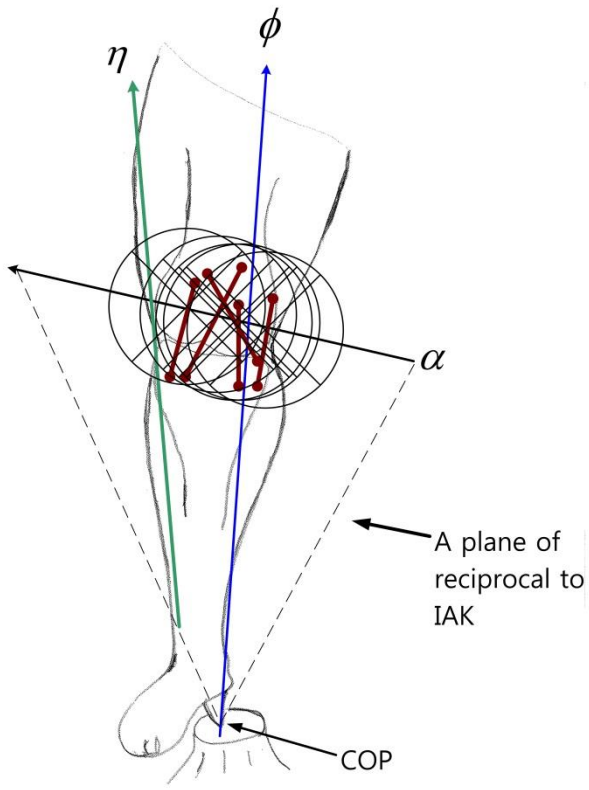

Figure 2. The knee joint provides the instantaneous screw α which is reciprocal to the impulsive ground reaction force ϕ. No combination of angular velocity about the α axis will cause instantaneous translational movement, while any force at the ground contact will not cause a rotation about α. The reaction forces (and torques) of the GRF will then be taken up by the musculoskeletal structures with the limb. Muscle contraction η and GRF ϕ are compounded into a wrench, which is limited to a plane of COP and reciprocal to the IAK. The reciprocal forces reside in the plane is resolved into component wrenches belonging to the reciprocal screw system of the five components as indicated in the Figure 1. (Adapted from the original figure published in Kim et al. [15].)

conditions. Thereby, during level walking, the active muscle shortens only a little and performs little works but provides the forces necessary to support body weight economically [30].

The instantaneous axes of the knee (IAK) are reciprocal to five constraints: the anterior cruciate ligament (ACL), the posterior cruciate ligament (PCL), the medial collateral ligament (MCL), and articular contacts in both the medial (P_1) and lateral (P_2) compartments of the knee (Figure 1). The reaction of the five constraints, which limit the motion of the knee, will neutralize every wrench on a screw that is reciprocal to the IAK. To affect the movement along the IAK against forces at the constraints, which are reciprocal to the IAK, no work will be required.

We found that if the IAK is given, and a location of the COP (center of pressure) on the axis of the GRF is known, then the GRF vector is limited to a plane in the screw system of the first order [31] (Figure 2). This aligns the knee joint with the GRF such that the reaction torques are eliminated. The reaction to the GRF will then be carried by the musculoskeletal structural components of the knee instead, thus representing the stationary configuration of the knee [29]. We established a framework for the estimation of the reaction constraints about the knee, including the *in vivo* medial and lateral contact forces, using a process that was simplified by the judicious generation of the IAK for the first order of freedom during equilibrium.

When the IAK is reciprocally connected to the GRF during the stance phase of movement, the knee joint can be considered to be in a state of reciprocal configuration. A considerable GRF can be exerted during the stance phase of the leg within the gait cycle when the axis of said GRF nearly coincides with a reciprocal screw. This stationary configuration within the stance phase is important because the knee can then exert a wrench of substantial intensity on the corresponding reciprocal force vector, without engendering an overload of any of the muscles that contribute to the torque about the knee [29].

2.2 Informational framework

The foundation of our computational framework is a perception-action coupling manifold connecting knee kinematics to the ground reaction vector in the sense of the reciprocal connection. The principle of virtual velocities states if the knee is in equilibrium then the work conducted during small displacements against the external forces must be zero.

We previously indicated that the ligaments and cartilage contacts of the knee joint contribute to its mechanical constraints [24]. We now need to prove if a knee has a freedom of the first order, then there is always one (and only one) screw φ for the GRF that determines the DOF of the knee. Thus a kinetic impulsive wrench on the knee will create a given screw α as the instantaneous screw axis (ISA) within the IAK [14].

Importantly, perception-action coupling manifold, which utilizes correlating alignments of both the generating lines of IAK and GRF, can be used to investigate how an individual perceive affordances for effective locomotion [18]. Perception-action coupling manifold is a purely geometric representation of the patient-ground interaction.

Plücker [32, 33] showed if any screw motion about a certain axis be given to the acting force lines forming a linear complex, then these force lines still remain within the complex. Hence, if all lines of a complex are subjected to a screw motion about the axis, then the complex itself is not altered. We thus see if a knee having freedom of the first order is in equilibrium, then the forces that act upon the body shall re-

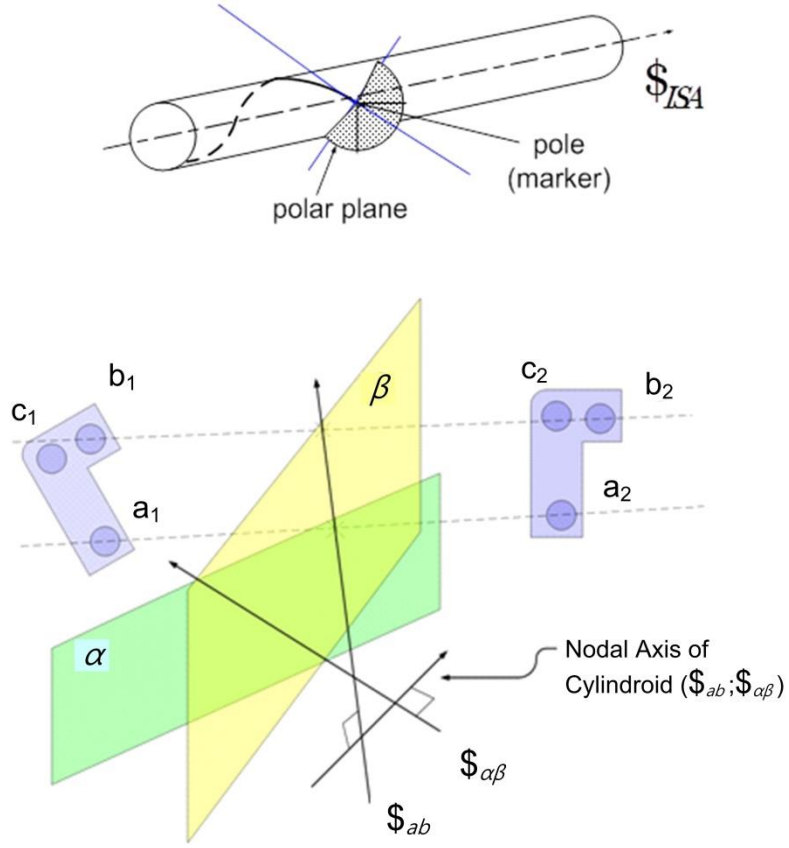

Figure 3. A special line complex is that defined by a single twist $\$_{ISA}$. Every marker point of the segment has its velocity vector tangential to the helix that passes through it. The pattern of this velocity vector is a helicoidal velocity field. Each marker point that does not coincide with the twist axis of $\$_{ISA}$ is referred to as a pole. Associated with each pole is its corresponding polar plane. Shown are a polar plane and its corresponding pole as defined by the instantaneous screw axis $\$_{ISA}$. The ISA $\underline{\$}_{ISA}$ used to transform the marker set (a_1, b_1, c_1) to (a_2, b_2, c_2) must be determined from cylindroids ($\$_{ab}$; $\$_{\alpha\beta}$). $\$_{\alpha\beta}$ and $\$_{\alpha\beta}$ are two twists of zero pitch on the cylindroid ($\$_{ab}$; $\$_{\alpha\beta}$).

side within these line complexes in a screw system of the fifth order. This system is in-turn reciprocal to the screw, which defines the degree of freedom, without ceasing to belong to the complex.

An algorithm has been used to estimate the linear complex at each coordinate, as defined at the surface marker points [34]. This approach will facilitate the analysis of displacements between two generally disposed axes and employ cylindroidal coordinates to denote this quantity [15]. A line complex is defined as a three-parameter family of lines. One form of the line complex that has significance with regard to the ISA ($\$_{ISA}$) is the linear line complex [34-36]. Such a line complex consists of the lines that are perpendicular to a family of curves. The latter family of curves is a helix defined by a single screw. The reason for this particular form is that the velocity vector of a body marker is tangential to the helix that passes through the markers. Lines through marker coordinates that are normal to the tangent vector along the trajectory at the markers are called path normals (Figure 3). Their Plűcker coordinates satisfy a linear equation:

$$o = [\Delta][\$_{ISA}]^T[\$] \tag{1}$$

which determines the linear line complex, defined by the instantaneous screw axis $\$_{ISA}$. A useful interchange operator is now introduced [37]:

$$[\Delta] = \begin{bmatrix} o & [I_3] \\ [I_3] & o \end{bmatrix} \tag{2}$$

Essentially, a six-by-six matrix is defined so that each submatrix $[I_3]$ is the three-by-three identity matrix, and the dots indicate two three-by-three arrays of zeros that fill out the matrix.

Conversely, any linear complex, defined by the screw $\$_{ISA}$, executes a helicoidal trajectory. It is thus formed by the path normals, defined as $, of screw motion. Coincident with each pole (marker coordinate) is a unique plane perpendicu-

lar to the helix. This plane is referred to as a polar plane relative to the twist $\$_{ISA}$.

Three markers a_1, b_1 and c_1 in the initial configuration and their corresponding Cartesian point coordinates a_2, b_2 and c_2 in the second configuration were used to derive linear complexes (Figure 3). Line A was then determined by the joint of the two points a_1 and a_2. Similarly, two additional lines B and C were determined by the joints of the points b_1 and b_2, and c_1 and c_2, respectively. The two lines or zero pitch screws $\$_{ab}$ and $\$_{\alpha\beta}$ are referred to as a pair of conjugates, whose polar properties, like those of the conics, follow Joachimsthal's equation [21, 38] and do not belong to lines of the linear complex. The central axis of the linear complex is the ISA, which is determined by the linear combination of two twists; hence if all the lines of a complex are subjected to a screw motion about this central axis, the complex itself is not altered. The polar plane α perpendicular to the line A exists at the pole $r_a = (a_1 + a_2)/2$. Similarly, two additional Polar planes, β and γ and their corresponding poles, exist. The three polar planes α, β, and γ and their corresponding poles r_a, r_b and r_c determine a linear complex.

To map point a_1 to a_2 via pure rotation, the axis of rotation must reside in the polar plane α. In a similar way, the mapping of point b_1 to b_2 via a rotation only must occur about an axis that resides in the polar plane β. The only axis that satisfies these two restrictions is the line of intersection $\$_{\alpha\beta}$ determined by two polar planes α and β. The next step is to displace point c_1 to c_2 without disturbing the mapping of points a_1 and b_1 to a_2 and b_2, respectively. This is achieved by a pure rotation about the line $\$_{ab}$ joining the two poles r_a and r_b.

The $\$_{ISA}$ is determined by the linear combination of two twists of zero pitch, $\$_{\alpha\beta}$ and $\$_{ab}$. Hence the twist $\$_{ISA}$ is on the cylindroid $(\$_{ab}; \$_{\alpha\beta})$. Given the two zero pitch screws $\$_{ab}$ and $\$_{\alpha\beta}$, we locate their common normal and let the one associated with the principal coordinate system lie along this nodal line. We can recognize that all screws of the cylindroid are perpendicular to the nodal line. The two lines $\$_{ab}$ and $\$_{\alpha\beta}$ are referred to as a pair of conjugates, indicating orthogonality [22]. Another cylindroid $(\$_{bc}; \$_{\beta\gamma})$ is defined by the two transversals $\$_{\beta\gamma}$ and $\$_{bc}$.

The $\underline{\$}_{ISA}$, the free vector component of the $\$_{ISA}$, is determined by recognizing that the only direction perpendicular to the nodal axes of the two cylindroids $(\$_{ab}; \$_{\alpha\beta})$ and $(\$_{bc}; \$_{\beta\gamma})$ is

$$\underline{\$}_{ISA} = \frac{(\underline{\$}_{ab} \times \underline{\$}_{\alpha\beta}) \times (\underline{\$}_{bc} \times \underline{\$}_{\beta\gamma})}{\left\|(\underline{\$}_{ab} \times \underline{\$}_{\alpha\beta}) \times (\underline{\$}_{bc} \times \underline{\$}_{\beta\gamma})\right\|} \tag{3}$$

The ISA of $\$_{12}$ is the intersection between two cylindroids $(\$_{ab}; \$_{\alpha\beta})$ and $(\$_{bc}; \$_{\beta\gamma})$ such that

$$\$_{ISA} = \$_{ab} + k\$_{\alpha\beta} \tag{4}$$

where the twist amplitude ratio k is determined by crossing the free vector part $\$_{ab} + k\$_{\alpha\beta}$ into $\$_{ISA}$.

With a twist of small amplitude about the ISA, the marker is moved to an adjacent point (Figure 3). To affect this movement against a force at the marker which is perpendicular to the line joining the two points, no work will be required; hence every line through the marker, perpendicular to the line, may be regarded as a screw of zero pitch, reciprocal to the ISA.

2.3 Computer-aided planning structing a patient-specific knee model

The key to understanding the knee joint is the realization that its movement is helicoid in character; the knee is not a simple hinge joint [39]. This screw-action of IKA gives to any position of the knee joint a stability that would be denied with a straight up-and-down hinge joint. It also follows that the reactions of the constraints in the medial and lateral contact are only manifested by the success with which they resist the stance phase of foot loading to disturb the equilibrium of the knee.

As a validation of this approach, we have accessed the 'Grand Challenge Competition to Predict in vivo Knee Loads' study which produced a series of comprehensive publicly available in vivo data sets for evaluating musculoskeletal model predictions of contact and muscle forces in the knee. To validate our specific knee model as a therapeutic approach addressing the IAK during the stance phase of gait, we compared our output with the published experimental data sets [40] generated for the medial and lateral contact forces. The available quantitative information included motion capture kinematics, fluoroscopy data, ground reaction forces, electromyographical (EMG) data, as well as the medial and lateral knee contact forces [40]. Data were collected from an instrumented right total knee replacement in an adult male subject (subject JW, mass 65 kg, height 1.7 m). The gait trial for said subject demonstrated a medial-lateral trunk sway gait pattern. Our study then used the following protocol to predict reaction of constraints (Figure 4). The inputs into the reciprocally connected knee model included experimental kinematics (x-y-z trajectories of surface marker data acquired at the patella, shank and thigh) and joint reaction forces that were obtained from the instrumented right knee of the subject. A knee radiograph contained a view of the knee region in the frontal plane and provided geometrical information about the ligament and contact surface constraints. In Step 1, the subject data were used to generate the ISA of the shank and thigh. In Step 2, the three-axis theorem [35] was used to obtain the ISA of the knee joint, i.e., the IAK, from two axes that had previously been obtained. In Step 3, the reciprocally connected knee model was used to locate a set of screw axes associated with contact forces that were reciprocally connected to the IAK. Then, we tested our computational framework by comparing the measured with the predicted knee medial and lateral contact forces.

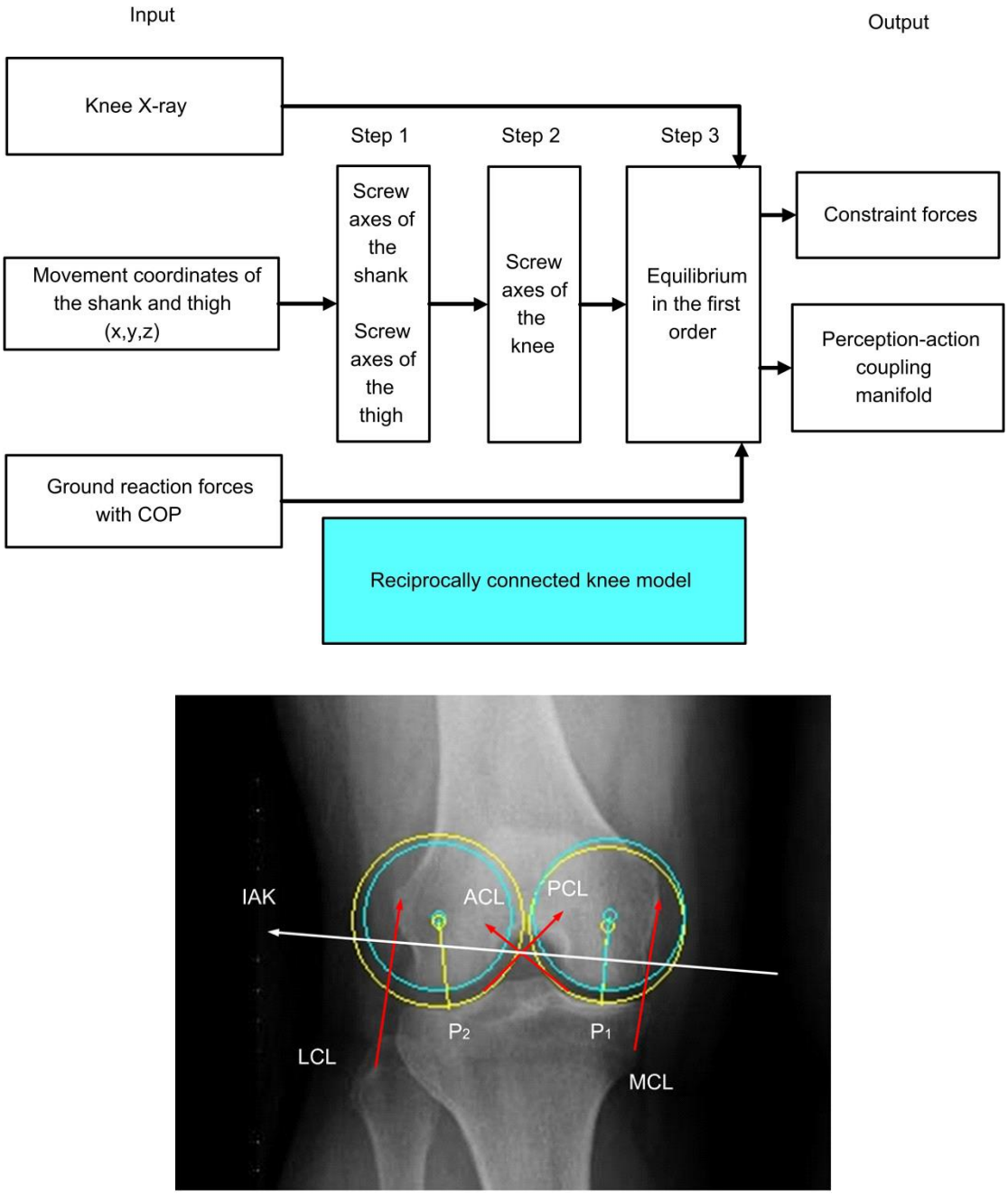

Figure 4. An illustration of the computational framework used to predict constraint forces for the presented knee model. The reactions of the five constraints, which limit the motion of the knee joint, are shown as an overlay of a radiographic image. These reactions will neutralize every wrench on a screw in the constraint manifold that is reciprocal to the IAK. Thus, no work will be required to affect the movement along the IAK against forces at the constraints, which are reciprocal to the IAK. (Adapted from the original figure published in Kim et al. [15].)

As an imaging complement to the knee model, the fiber tractography of a portion of the gastrocnemius lateralis muscle was generated in a healthy subject. The images were generated with one region of interest, correspondent to the muscle boundaries where the anatomical cross-section area was maximal. The subject was examined in a whole-body magnetic resonance imaging scanner (Signa HDxT 1.5T, GE Healthcare, USA). The subject was placed in the supine position with feet first and care was taken to position the subject with the long axis of the leg placed parallel to the magnetic field. The right shank was imaged using diffusion tensor imaging and gradient-echo T2 sequences [41]. Then muscu-

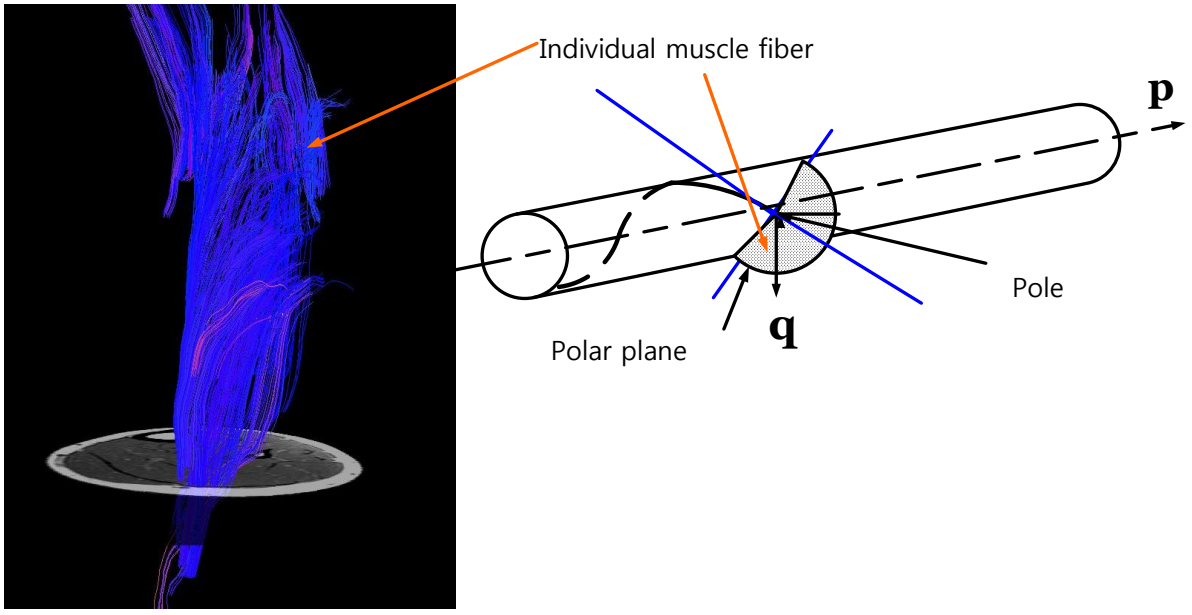

Figure 5. Fiber tractography imaging of a portion of the gastrocnemius lateralis muscle generated in a healthy subject. The images were generated with one region of interest, correspondent to the muscle boundary where the anatomical cross-section area was maximal. The subject's leg was placed parallel to the magnetic imaging field. The pole and pole plane within a single muscle fiber are shown. (Adapted from the original figure published in Kim et al. [15].)

lar tractography was performed on each muscle. Our study demonstrated the feasibility of providing *in vivo* three-dimensional architecture of the human shank muscles using tractography from medical imaging and of determining muscular microstructural parameters.

With legs in a relaxed position, we have not used the image acquisition to actually identify the line complex for the individual fiber during motion; rather we have introduced the exemplar image to describe a method by which a population of motor neurons could determine, uniquely the direction of IKA in three-dimensional pace [42].

3. Results

Results from tractography imaging indicated a manifold of fibers associated with knee stability (Figure 5). When contracted, the fibers represent a linear line complex defined by a single twist $\boldsymbol{P}$. Every point of the fiber segment has a velocity vector, which is tangential to the helix that passes through it. The pattern of this velocity vector is a helicoidal velocity field. Each point that does not coincide with the twist axis of $\boldsymbol{P}$ is referred to as a pole. One geometric component associated with each pole is its corresponding polar plane. A polar plane and its corresponding pole were defined by the instantaneous screw axis $\boldsymbol{P}$ within an individual fiber.

A typical gait pattern from our model can be graphically visualized in terms of two sets of ISAs, which are defined as $\$_1$ (Figure 6(a) for the shank) and $\$_2$ (Figure 6(b) for the thigh). At the beginning of the stance phase, the typical gait pattern produced the typical shape of ISA generated with small motion increments (0.23° to 0.46°) of the shank and thigh in the transverse plane (the first axis, indicated by the '1' in Figures 6(a) and 6(b)). The motion pathways of the shank showed distinctive profiles that were characterized by an excursion of axes in a flattened shape, while the ISAs of the thigh were in a rounded shape. Both of the ISA's were represented relative to the global reference frame. The dynamic IAK was determined by the linear combination of two ISA's of the shank and thigh (Figure 7). Moreover, by virtue of the IAK's position in the global frame, an IAK could be connected with the GRF existing on the screws during gait [43]. The issue of relating the reciprocal connection corresponding between impulsive forces such as the GRF and IAK (zoomed in sub-figure in Figure 7), adds an additional component to facilitate this parity (which has not yet been reported in terms of the ISA). Therefore, a one-to-one correspondence via the perception-action coupling manifold exists between the impulsive reaction forces and the instantaneous screw, or to express this differently, the complex of instantaneous and impulsive screws are projective.

In the model presented in this paper, the first order freedom equilibrium condition was considered so that a knee is only free to twist about IAK. A given GRF may be replaced by a wrench of appropriate intensity on any muscle. Both the GRF and wrench are compounded into an alternative wrench, which is reciprocal to the IAK and resolved into component wrenches belonging to the reciprocal screw system (shown here as the lateral and medial contact forces in Figures 8 and 9, respectively). The instrumented knee data for the trunk-

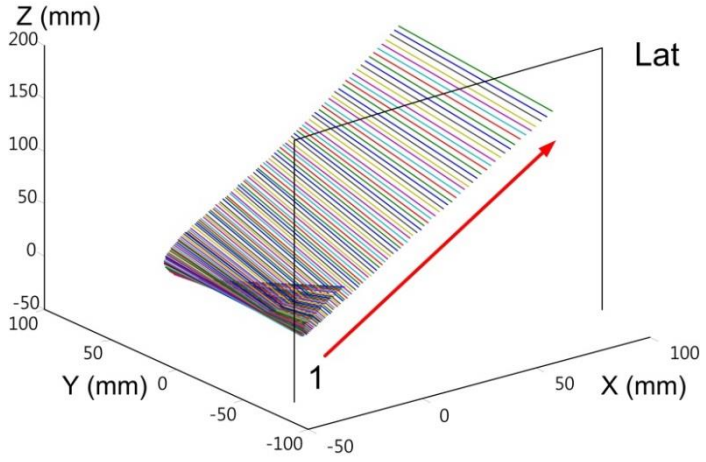

(a)

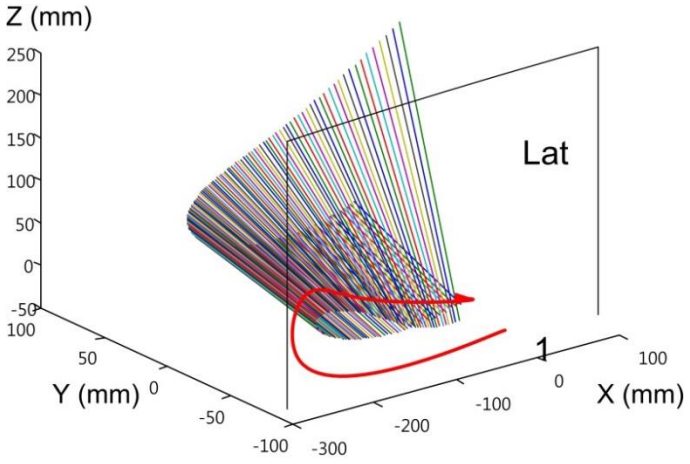

(b)

Figure 6. A three-dimensional view of the instantaneous screw axes (ISA) from the postero-medial side of the shank (a) and the thigh (b). The endpoints of the axes are at the intersections with medial and lateral 'Lat' sagittal planes, located -60 mm to 60 mm off the origin of the global frame. The first axis, indicated by the '1', represents the first step of the *ISA*. The red arrow indicates the path along which each new axis migrates at every subsequent 0.05 second increment. (Adapted from the original figures published in Kim et al. [13] and Kim et al. [29].)

sway gait trials for the data sets were compared to the model prediction. The predicted maximum medial contact force was 1,092.0 N, scaled to subject's body weight (BW) as 1.7 (Figure 9). The maximum in vivo medial contact force that was reported ranged from 1.2 to 2.0 BW, typically remaining between 1.2 and 1.7 BW [40]. The root mean square (RMS) errors during the contact of the foot with the ground were observed as 148.1 N and 147.3 N for the lateral and medial, respectively, over the entire stance phase.

4. Conclusions

The purpose of this paper was to review the application of a perception-action coupling manifold connecting the instantaneous screw to the GRF in the estimation of reaction of constraints. By the careful generation of the knee ISA, the zero work constraints are connected to the IAK with their virtual work being automatically zero. Then only the muscle forces are needed to equilibrate with the GRF, since they are excluded from the constraints that are reciprocal to the IAK. The coupling manifold is easy to understand and implement

in the sense of a simplified computational framework. We have demonstrated a perception-action coupling manifold, that was generated in terms of two screw-axis surfaces during the stance phase can explain the interaction between gait kinematics and applied external forces. Therefore, the shape of the reciprocal condition in the perception-action coupling manifold can be regarded as the minimal unit of analysis of a gait pattern under all load-bearing physiological conditions. As reported here, there exists a unique one-to-one correspondence between the GRF and the IAK. The unique characteristic of the GRF-IAK relationship and application may suggest a new field for physiotherapy investigation. It is of interest to see progress in the clinical implications of a patient-specific basis or personalized medicine regarding therapeutic approaches to gait disorders.

We have enunciated that if a knee joint has a freedom of the first order in equilibrium, then the necessary and sufficient condition is that the forces which act upon the joint shall constitute a wrench on a screw of the screw system of the fifth order [13]. This wrench is then reciprocal to the screw, which defines the freedom of the knee joint. We thus see that every straight line in space may be the residence of a screw, a wrench on which is consistent with the equilibrium of the body. We demonstrated that the muscle synergy is equivalent to a complex of lines, a manifold approximated by individual fibers. We then see during level locomotion, that the active muscle has little shortening and performs little work but provides the force necessary to support body weight economically. Locomotion economy is improved by muscles that act as active struts rather than working machines [30].

Since concurrent activation of muscles due to disturbances during gait has to be compounded into the reciprocal screw system, these forces would be neutralized by the reactions of the constraints, which in-turn would increase those reactions. This feature stands in contrast to many modern computational approaches in which the feedback and feed forward controller gains in muscle activation [17]. These approaches do not necessarily have any biophysical meaning, but represent a control optimization scheme driving the kinematic trajectories of the models toward experimentally obtained trajectories [44]. It also follows that the reactions of the constraints by which the movements of the knee are confined to twist about the screws of the IAK can only be wrenches on the reciprocal screw system of the fifth order. The reactions of the constraints are only manifested by the success with which they resist the efforts of certain wrenches, i.e., applied GRF, which disturb the equilibrium of the knee. The conventional approaches typically only consider the reaction of the constraints, which limit the vargus/varus rotation of the knee. In this case, the impulsive reaction of the constraints due to the impulsive muscle forces on which would, if the knee were perfectly free, cause an instantaneous motion about the IAK were not included. The contact forces are generally determined using static equilibrium about the adduction/abduction moment in the tibial frontal plane [6].

There were similarities between the prediction of this mod-

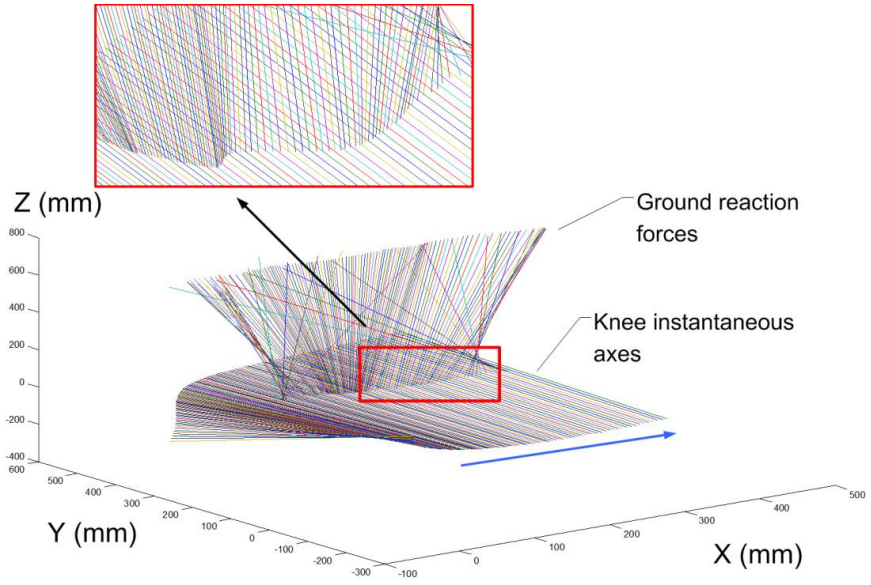

Figure 7. In a verification of the IAK tracking during a time-sequence of motion data, the knee ISA screws are shown to nearly coincide with a reciprocal screw of the GRF as indicated in the zoomed in panning view. This representative analysis indicates a perception-action coupling manifold. This manifold is a special configuration that can exert a wrench of substantial intensity on the corresponding reciprocal screw in the GRF without overload of torque on the knee joint. The blue arrow indicates the gait pathway. (Adapted from the original figure published in Kim et al. [14].)

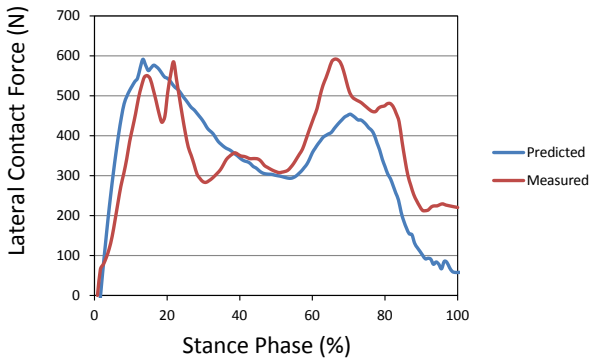

Figure 8. A comparison between the results of our theoretical approach and data gathered from an instrumented knee during gait trials [40]. Predicted and Measured values of constraint forces at the lateral contact are comparable with an RMS error = 148.1 N. Results were originally published in Kim et al. [15].

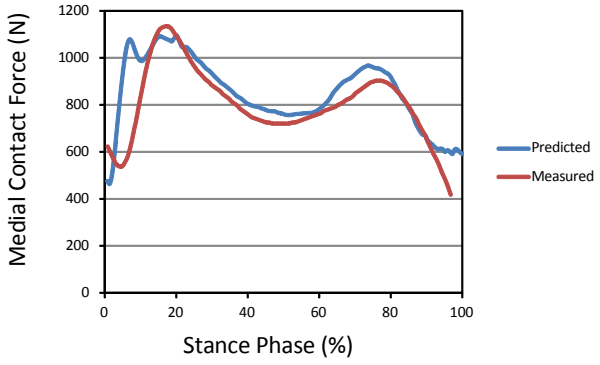

Figure 9. A similar comparison between the results of our theoretical approach and data gathered from an instrumented knee during gait trials [40]. Predicted and Measured values of constraint forces at the medial contact are comparable with RMS error = 147.3N. Results were originally published in Kim et al. [15].

el and a previous study [45], the goal of which was to identify how individual muscles contribute to the axial tibiofemoral joint force. In our study, the knee joint loading pattern during the stance phase indicates two major peak force levels, the first peak occurring early within the stance phase and the second peak occurring later in the gait cycle (Figures 8 and 9). Here the medial compartment bears a greater proportion of the net load than the lateral compartment. Slight differences between predictions in our method and the instrumented joint data by were also observed [40, 45]. The extent to which discrepancies occurred between the predicte d and actual values for the contact forces can be attributed to the fact that our modeling approach did not include the customary full-body computer model and the analysis was performed from merely knowing the order of the DOF which is mandated by the constraints. However, the central question to this paper is not whether the contact forces could be predicted accurately in human locomotion, but whether information for controlling locomotion is available and applied during the stance phase. Contact forces generally receive primary attention because conventional studies relate these with pathological conditions. Here we replaced these contact forces with a perception-action coupling manifold as operationalized parameters. We introduced this concept in order to create and control manifolds from theoretically justified state variables [46].

It is important to realize that inverse dynamic models calculate the joint reaction forces on the basis of the assumption that the knee joint is a hinge joint and that the moment of force is generated by a torque motor [47]. In reality the knee joint does not have any resemblance of a rotary actuator; rather it is moved by an elaborated system of the five variables mentioned, a reciprocal screw system and muscles [24]. Correct resolution of the muscle forces into constraints has important implications for accurate calculation of articular contact forces, since muscle contraction increases contact force [40].

We demonstrated how the impulsive reactions of the constraints are determined through the reduced wrench. In the most general case when a wrench on the GRF is not along the reciprocal screw, the reaction torques on the knee must compound into a wrench ρ, which is reciprocal to the IAK. The component wrenches of ρ on this reciprocal system must be neutralized by the reaction of the constraints, thus resulting in larger loading of the constraints [13]. Therefore, we propose that the screw axis surfaces presented in the perception-action coupling manifold are less influenced by tuning parameters and may be the basis of gait-related disorders. We also propose that the screw axis surfaces are the basis of, or allow for, the identification of a subject-specific gait signature. The configuration of ISAs of the knee as related to their corresponding GRFs has not been reported previously and has not been considered as an important element for gait disorder diagnosis and therapy. We note, however, that in the automobile industry it has been proposed that the ISA surfaces representing a vehicle's suspension may be included in the vehicle's dynamic performance index [48]. It has been reported that current vehicle dynamic performance indices that primarily depend on multibody dynamic tools appear to be insufficient in representing the fundamental vehicle performance because of the influence from tuning elements such as springs.

Our linear complex method differs from the coordinate transformation approach in so far as it can directly generate the ISA from markers whose coordinates are both conveniently measurable and referenced to the GRF, and independent of the coordinate system. The linear complex approach is typically less popular than coordinate transformation. How-

ever, its unique feature, i.e., where acquired motion capture data are directly applicable, could provide the positioning of the IAK with reference to the corresponding GRF.

This study is limited in so far as we have only presented case study data. We therefore suggest several areas for future research: 1) further testing of patients with various gait disorders, and physical activity levels of knee to better understand the interaction between knee kinematics and *in vivo* loading during gait; 2) inclusion of more accurate knowledge of structural components representing the constraints; and 3) the exploration of how computational technology available for ISA and GRF determination may be transferred into improvements in applied clinical practice. These improvements may include the effectiveness of clinical planning in support of both patients and their clinicians in order to optimize treatments across a wide range of gait profiles and physical levels.

In conclusion, the reviewed computational technique characterizes the dynamic alignment of *in vivo* knee loading. The approach demonstrates the alignment of the IAK associated with the GRF reducing the payload on the medial/lateral compartments, thus transmitting the reaction (braking) torque to the structure of the limb. This alignment then eliminates the internal reaction (braking) torques and forces within the joint. Special orthotic or orthopedic treatments, which are rich in addressing the reciprocal configuration phenomenon, may be designed for the post-treatment outcome of gait-related disorders. An optimized treatment applying this approach requires further investigation. Overall, the essential geometric character of this novel method seems particularly well adapted to provide an ecological solution for individual variations. Thus a simplified framework has been described here as a viable foundation for making gait analysis more clinically useful through diagnostic specificity.

Acknowledgments

Author WK extends his thanks to Ms. Cristina Monleón García of Universidad Católica de Valencia, an enthusiastic dancer, for her inspiration in this study. Author WK also thanks his daughter, April Kim, and son, Dennis Kim, for their continuous encouragement of this research. The experimental data, used for validation of the model, were provided by the Grand Challenge Competition to Predict In Vivo Knee Loads as part of the Symbiosis project funded by the National Institutes of Health (Grant U54 GM072970). Author SSK acknowledges partial support from the US Air Force Materials Directorate through a subcontract with Clarkson Aerospace Corporation (PI: Dr. Yu Liang, Contract FA8650-05-1912) and from the US Air Force Research Laboratory (PI: Dr. Kimberly D. Kendricks, Contract SOO Task Number 18 and Topic Title: 3.2.2.2.4 Human Centric ISR Sensors), both provided as subawards from Central State University (Ohio).

References

[1] Chao EYS, Sim FH. Computer-aided preoperative planning in knee Oosteotomy. The Iowa Orthopaedic Journal.1995; 15(1): 4-18.

[2] Shah M, Spilker R, Koff MF, Lipman J. Patient specific three dimensional knee model. In: 2011 IEEE 37th Annual Northeast Bioengineering Conference **(**NEBEC 2011**)**; 2011 April 1-3; Troy, NY; p.1-2.

[3] Garg A, Walker PS. Prediction of total knee motion using a three-dimensional computer-graphics model. Journal of Biomechanics. 1990; 23(1): 45-58.

[4] Martelli S, Ellis RE, Marcacci M, Zaffagnini S. Total knee arthroplasty kinematics: computer simulation and intraoperative evaluation. The Journal of Arthroplasty. 1998; 13(2): 145-155.

[5] Delp SL, Anderson FC, Arnold AS, Loan P, Habib A, John CT, Guendelman E, Thelen DG. Opensim: open-source software to create and analyze dynamic simulations of movement. IEEE Transactions on Biomedical Engineering. 2007; 54(11): 1940-1950.

[6] Gerus P, Sartori M, Besier TF, Fregly BJ, Delp SL, Banks S A, Pandy MG, D'lima DD, Lloyd DG. Subject-specific knee joint geometry improves predictions of medial tibiofemoral contact forces. Journal of Biomechanics. 2013; 46(16): 2778-2786

[7] Steele JR, Basu A, Job A. A three-dimensional representation of an athletic female knee joint using magnetic resonance imaging. Medical Engineering and Physics. 1994; 16(5): 363-369.

[8] Neptune RR, Clark DJ, Kautz SA. Modular control of human walking: a simulation study. Journal of Biomechanics. 2009; 42(9): 1282-1287.

[9] Neptune RR, Mcgowan CP, Fiandt JM. The influence of muscle physiology and advanced technology on sports performance. Annual Review of Biomedical Engineering. 2009; 11: 81-107.

[10] Neptune RR, Mcgowan CP, Kautz SA. Forward dynamics simulations provide insight into muscle mechanical work during human locomotion. Exercise and Sport Sciences Review. 2009; 37(4): 203-210.

[11] Ting LH, Mckay JL. Neuromechanics of muscle synergies for posture and movement. Current Opinion in Neurobiology. 2007; 17(6): 622-628.

[12] Todorov E. Optimality principles in sensorimotor control. Nature Neuroscience. 2004; 7(9): 907-915.

[13] Kim W, Veloso AP, Araújo D, Vleck V, João F. An informational framework to predict reaction of constraints using a reciprocally connected knee model. Computer Methods in Biomechanics and Biomedical Engineering. 2013; 1-12. DOI: 10.1080/10255842.2013.779682

[14] Kim W, Kim YH, Veloso AP, Kohles SS. Tracking knee joint functional axes through Tikhonov filtering and Plűcker coordinates. Journal of Novel Physiotherapies. 2013; 4(1): 11732. DOI: 10.4172/2165-7025.S4-001

[15] Kim W, Espanha M, Veloso A, Araújo D, João F, Carrão L, Kohles SS. An informational algorithm as the basis for perception-action control of the instantaneous axes of the knee. Journal of Novel Physiotherapies. 2013; 3(127): 2.

[16] Kim W, Veloso A, João F, Kohles SS. Efferent copy and corollary discharge motor control behavior associated with a hopping activity. Journal of Novel Physiotherapies. 2013; 3(167): 2.

[17] Kim W, João F, Tan J, Mota P, Vleck V, Aguiar L, Veloso A. The natural shock absorption of the leg spring. Journal of Biomechanics. 2013; 46(1): 129-136.

[18] Gibson JJ. The ecological approach to visual perception. Psychology Press; 1986. 332 p.

[19] Kim W, Tan J, Veloso A, Vleck V, Voloshin AS. The natural frequency of the foot-surface cushion during the stance phase of running. Journal of Biomechanics. 2011; 44(4): 774-779.

[20] Reed ES. Issues in the Ecological Study of Learning. Hillsdale (NJ): Psychology Press; 1985. Chapter 13, An ecological Approach to the evolution of behavior; p. 357-386.

[21] Ball RS. A treatise on the theory of screws. Cambridge University Press; 1900. 544 p.

[22] Ball RS. A treatise on the theory of screws. Re-issue. Cambridge University Press; 1998. 544 p.

[23] Hunt KH. Kinematic geometry of mechanism. Oxford University Press; 1990. 465 p.

[24] Kim W, Kohles SS. A reciprocal connection factor for assessing knee-joint function. Computer Methods in Biomechanics and Biomedical Engineering. 2012; 15(9): 911-917.

[25] Kim W, Veloso A, Araújo D, Machado M, Vleck V, Aguiar L, Cabral S, Vieira F. Haptic perception-action coupling manifold of effective golf swing. International Journal of Golf Science. 2013; 2(1): 10-32.

[26] Teu KK, Kim W, Fuss FK, Tan J. The analysis of golf swing as a kinematic chain using dual euler angle algorithm. Journal of Biomechanics. 2006; 39(7): 1227-1238.

[27] Turvey MT, Romaniak-Gross C, Isenhower RW, Arzamarski R, Harrison S, Carello C. Human odometer is gait-symmetry specific. Proceeding of the Royal Society B: Biological Sciences. 2009; 276(1677): 4309-4314.

[28] Berkeley G. An essay towards a new theory of vision. Rockville (MD): Arc Manor; 2008. 92 p.

[29] Kim W, Veloso AP, Vleck VE, Andrade C, Kohles SS. The stationary configuration of the knee. Journal of the American Podiatric Medical Association. 2013; 103(2): 126-135.

[30] Roberts TJ, Marsh RL, Weyand PG, Taylor CR. Muscular force in running turkeys: the economy of minimizing work. Science. 1997; 275(5303): 1113-1115.

[31] Möbius A. Ueber die Zusammensetzung unendlich kleiner Drehungen. Journal für die reine und angewandte Mathematik. 2009; 1838(18): 189-212.

[32] Jessop CM. A treatise on the line complex. Cornell University Press; 1903. 382 p.

[33] Plücker J, Klein F. Neue Geometrie des Raumes gegründet auf die Betrachtung der geraden Linie als Raumelement. Erste-[Zweite] Abtheilung [Internet]. Ann Arbor (MI): University of Michigan Library; 1868 [cited 2005]. 378 p. Available from: http://name.umdl.umich.edu/ABN8081

[34] Dooner D, Seireg A. The kinematic geometry of gearing: a concurrent engineering approach. Wiley-Interscience; 1995. 472 p.

[35] Dooner DB. On the three laws of gearing. Journal of Mechanical Design. 2002; 124(4): 733-744.

[36] Huang C, Ravani B, Kuo W. A geometric interpretation of finite screw systems using the bisecting linear line complex. Journal of Mechanical Design. 2008; 130(10): 102303.

[37] Lipkin H, Duffy J. Hybrid twist and wrench control for a robotic manipulator. Journal of Mechanisms Transmissions and Automation in Design. 1988; 110(2): 138-144.

[38] Çöken AC, Görgülü A. On Joachimsthal's theorems in semi-Euclidean spaces. Nonlinear Analysis: Theory, Methods and Applications. 2009; 70(11): 3932-3942.

[39] Helfet A. Anatomy and mechanics of movement of the knee joint. In: Disorders of the knee. Philadelphia (PA): J.B. Lippincott; 1974; p. 1-17.

[40] Fregly BJ, Besier TF, Lloyd DG, Delp SL, Banks SA, Pandy MG, D'lima DD. Grand challenge competition to predict in vivo knee loads. Journal of Orthopaedic Research. 2012; 30(4): 503-513.

[41] Budzik JF, Le Thuc V, Demondion X, Morel M, Chechin D, Cotten A. In vivo MR tractography of thigh muscles using diffusion imaging: initial results. European Radiology. 2007; 17(12): 3079-3085.

[42] Georgopoulos AP, Kettner RE, Schwartz AB. Primate motor cortex and free arm movements to visual targets in three-dimensional space. II. coding of the direction of movement by a Neuronal Population. The Journal of Neuroscience. 1988; 8(8): 2928-2937.

[43] Fuller EA. Center of pressure and its theoretical relationship to foot pathology. Journal of the American Podiatric Medical Association. 1999; 89(6): 278-291.

[44] Thelen DG, Anderson FC. Using computed muscle control to generate forward dynamic simulations of human walking from experimental data. Journal of Biomechanics. 2006; 39(6): 1107-1115.

[45] Sasaki K, Neptune RR. Individual muscle contributions to the axial knee joint contact force during normal walking. Journal of Biomechanics. 2010; 43(14): 2780-2784.

[46] Kugler PN, Turvey MT. Information, natural law, and the self-assembly of rhythmic movement. Lawrence Erlbaum Associates; 1987. 416 p.

[47] Winter DA. Biomechanics and motor control of human movement. 4thed. Wiley; 2009. 384 p.

[48] Lee U. A proposition for new vehicle dynamic performance index. Journal of Mechanical Science and Technology. 2009; 23(4): 889-893.

[49] Bernstein NA. The co-ordination and regulation of movements. Pergamon Press; 1967. 196 p.